J. Fluid Mech. (1974), *vol.* 63, *part* 2, *pp.* 257–272
Printed in Great Britain

Shear fronts and an experimental stratified shear flow

By A. D. McEWAN AND P. G. BAINES

CSIRO Division of Atmospheric Physics, Station Street, Aspendale, Victoria 3195, Australia

(Received 20 June 1973)

The theoretical and experimental evaluation of a laboratory device for creating a controlled shear flow in a continuously stratified liquid is described. The shear is created by the movement of the end barriers of a rectangular channel. If these barriers are impulsively set into uniform shear motion, this motion propagates away in the form of a front of width $O((h/n)(Nt)^{\frac{1}{3}})$ travelling with uniform speed $Nh/n\pi$, where N is the (constant) buoyancy frequency, t is time, n is the vertical modal number and h is the channel depth. The shear produced has roughly twice the duration of that attainable using a tilting tube (Thorpe 1968) of similar dimensions. Shear enhancement is possible by introducing a properly designed flow contraction. If $N(z)$ is variable, the shear profile obtained is that appropriate to the lowest internal wave mode of infinite length.

1. Introduction

Not a great deal of experimental work has been done on the dynamics of stably stratified fluids in a vertical shear. This is possibly due to the difficulty of creating and sustaining the shear at a controllable and measurable level for a period sufficiently long to establish approximately steady conditions. In continuous flow devices such as those used by Moore & Long (1971) and Odell & Kovasznay (1971) the profiles of both density and shear are self controlled (i.e. by internal dynamics and not by the operator), with a resultant limitation in utility. Thorpe's (1968) tilting tube apparatus has the appeal both of simplicity and capacity for allowing the motion to be described accurately, but operating times are limited by the arrival of 'surge fronts' which proceed from each end of the tube as soon as tilting is commenced, and travel towards the centre at about the speed of a solitary wave.

Thermally stratified air has been used in other investigations such as those of Hewett, Fay & Hoult (1970) and Scotti & Corcos (1972). This provides the benefit of a continuously flowing system, but visualization and measurement are difficult to manage without disturbance, particularly at slow speeds; the higher kinematic viscosity of air limits the maximum Reynolds number attainable.

The apparatus described here is intended to extend, using water as the working medium, the operational time for controlled shear beyond that possible for a given amount of water in Thorpe's experiment. It does not permit the attainment

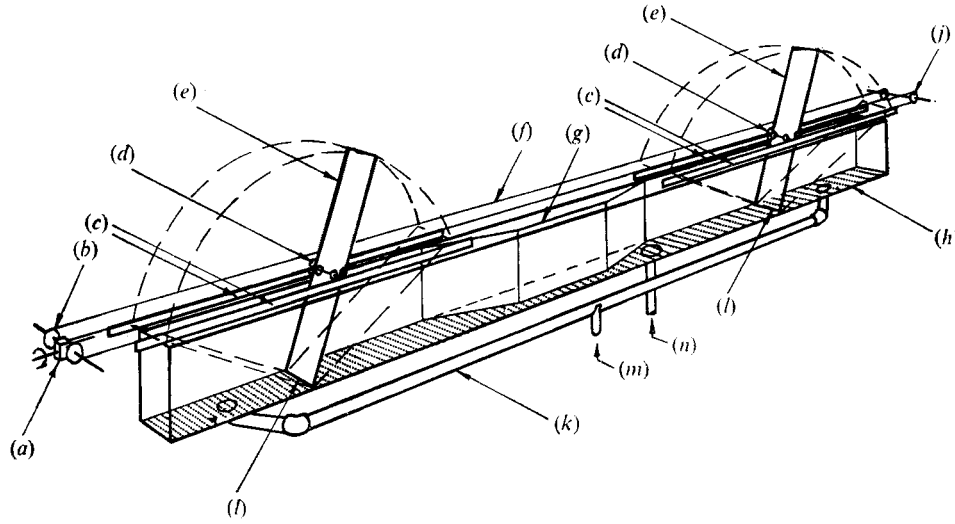

FIGURE 1. The apparatus. Notation is given in the text.

of Richardson numbers as low as those Thorpe achieved, but for the purpose of studying lee waves and critical-layer absorption it has some advantages, and it is currently being used in the investigation of these phenomena.

The accompanying theoretical discussion is intended not only as an aid to understanding the working of the device, but to provide some insight into the properties of solitary wave fronts propagating and reflecting within continuously stratified media.

2. Description of the apparatus

Reference is made to figure 1. In its present form the apparatus occupies a general-purpose 'perspex' sided tank (*h*) 5·49 m long, 0·228 m wide and 0·381 m deep, normally filled to a depth of 0·318 m with salt-stratified water.

At a distance of 0·914 m from one end a hinge (*l*) lies across the bottom of the tank, and attached to it is the lower edge of a paddle (*e*) which is long enough to occupy completely in any position the full width and depth of the tank. This paddle is sealed to the sides of the tank by a felt-coated rubber flap. Another flap seals the hinge, and there is thus formed a reasonably leak-free partition.

A second similarly located paddle occupies the opposite end of the tank, and these paddles are permanently located parallel to one another by means of guide roller assemblies (*d*) fitting over each plate and connected by steel cables (*f*).

The guide roller assemblies are constrained to travel in a plane above the tank and parallel to the tank bottom, by opposing rollers which engage tracks (*c*) (actually sliding door tracks) attached to the top of the tank frame. Steel cables on each side of the guide roller assembly extend horizontally above the tank to beyond the ends of the tank, where they pass over sheaves (*b*) and (*j*) fixed on horizontal shafts mounted transverse to the tank axis. One of these shafts is the output from a gearbox (*a*) driven by an electronically controlled d.c. motor.

Hence the paddles confine a rectangular parallelepiped of liquid whose base length and depth are constant, but within which the top plane may be sheared at a constant speed relative to the bottom.

The space confined at each of the outer ends of the tank is not constant in volume, but the net level of water contained there is maintained by connecting these spaces through a large bore (10 cm) pipe (k).

In preparation, the inner space is filled with stratified salt solution through a bottom mushroom opening (n) which is subsequently closed. For linear stratifications the two-tank method (Oster 1965) is used. Simultaneously the outer spaces are filled to the same level with fresh water, thus approximately equalizing the pressure across the plates and minimizing leakage of the stratified fluid. Once the tank is filled a monomolecular layer of cetyl alcohol is deposited on the free surface to inhibit evaporation. With care during filling the stratified fluid will remain virtually uncontaminated by the fresh water for several hours. Leakage past the paddle seals is greatest with the paddles in the inclined position, so during filling the paddles are preset upright.

In its present form the maximum shear velocity imposed on a free surface 0·318 m above the bottom is 5 cm/s and accurate control is possible down to 0·2 cm/s.

As shown in § 3 the maximum shearing rate within the fluid is $8/\pi$ times the paddle shear. This shear could be further increased by the insertion of a contraction (g) occupying the central section of the tank. This comprised a triangularly faired barrier mounted against one side wall to reduce the effective width of the tank. The contractions used for the results given here provided a reduced width for a distance of 0·61 m. The depth of the tank was unaltered.

3. The nature of the shear flow

The motion of each paddle as described above may be regarded as a horizontal translation of its mid-point (taken here to be at the half-depth of the fluid), plus a rotation about this mid-point, with a constant vertical shear. The translation results in a barotropic motion in the channel, set up by the propagation of small amplitude surface waves from the paddles when their motion commences. The oscillations associated with these waves decay rapidly and provided that the paddles move smoothly, the resultant barotropic motion is effectively steady.

Considering now the baroclinic motion, we assume that the fluid is in uniform translation from (say) left to right and take an origin situated at the bottom of the tank, below the mid-point of the left-hand paddle. With x and z horizontal and vertical co-ordinates and t the time variable, the linearized equations of motion, in the Boussinesq approximation, are

$$\left.\begin{aligned} \mathbf{u}_t &= -\nabla p/\rho_0 - \rho g\hat{\mathbf{z}}/\rho_0, \\ \nabla.\mathbf{u} &= 0, \quad \rho_t + w\, d\rho_0/dz = 0, \end{aligned}\right\} \tag{3.1}$$

where $\mathbf{u}$ is the vector fluid velocity and (u, w) its horizontal and vertical components, ρ is the perturbation density about the equilibrium density ρ_0, p the perturbation pressure, g the gravitational acceleration and $\hat{\mathbf{z}} = \nabla z$ is directed

upwards. The suffixes x, z and t denote partial derivatives. With a stream function ψ defined by

$$u = -\psi_z, \quad w = \psi_x, \tag{3.2}$$

we obtain

$$\nabla^2\psi_{tt} + N^2\psi_{xx} = 0, \tag{3.3}$$

where

$$N^2 = -(g/\rho_0)\, d\rho_0/dz. \tag{3.4}$$

We consider for the moment only one paddle, the end of a semi-infinite channel. The boundary conditions are

$$\left.\begin{aligned} w = \psi_x = 0, \quad & z = 0, 1, \\ u = -\psi_z = \begin{cases} 0, & t < 0, \quad x = 0, \\ \alpha(z - \tfrac{1}{2}), & t > 0, \quad x = 0, \end{cases} & \end{aligned}\right\} \tag{3.5}$$

where the effect of the paddle has been replaced by a representative velocity distribution at $x = 0$ (the effect of paddle inclination will be discussed below). α is the (constant) paddle shear and length dimensions are scaled by the tank depth h.

From (3.1), the initial conditions are

$$\psi = 0, \quad \nabla^2\psi_t = 0 \quad \text{as} \quad t \to 0. \tag{3.6}$$

The $x = 0$ boundary condition may be written as

$$u = \alpha(z - \tfrac{1}{2}) = \sum_{n=1}^{\infty} G_n \cos n\pi z = G(z), \tag{3.7}$$

where

$$G_n = \begin{cases} -4\alpha/n^2\pi^2, & n \text{ odd}, \\ 0, & n \text{ even}. \end{cases} \tag{3.8}$$

Taking the Laplace transform in the usual manner gives

$$\psi(x, z, t) = \frac{1}{2\pi i}\int_{\epsilon - i\infty}^{\epsilon + i\infty} e^{st}\, \Psi(x, z, s)\, ds, \tag{3.9}$$

where Ψ satisfies

$$\Psi_{zz} + \mu^2\Psi_{xx} = 0, \tag{3.10}$$

with

$$\epsilon > 0 \quad \text{and} \quad \mu^2 = 1 + N^2/s^2.$$

$$\Psi = 0, \quad z = 0, 1; \quad \Psi_z = -s^{-1}G(z), \quad x = 0. \tag{3.11}$$

These equations yield

$$\psi(x, z, t) = -\sum_{n=1}^{\infty} G_n \frac{\sin n\pi z}{n\pi} \frac{1}{2\pi i}\int_{\epsilon - i\infty}^{\epsilon + i\infty} \frac{e^{st}\, e^{-n\pi x/\mu}\, ds}{s}. \tag{3.12}$$

We now consider the integral

$$I(nx, t) = \frac{1}{2\pi i}\int_{\epsilon - i\infty}^{\epsilon + i\infty} \frac{e^{st} e^{-n\pi x/\mu}\, ds}{s} = \frac{1}{2\pi i}\int_{\epsilon - i\infty}^{\epsilon + i\infty} e^{tf(s)}\, ds, \tag{3.13}$$

where, if $x = Vt$,

$$f(s) = s - n\pi V/(1 + N^2/s^2)^{\frac{1}{2}} - t^{-1}\log s. \tag{3.14}$$

Assuming that t is large, the saddle points of the integrand are given by

$$f'(s) = 0, \tag{3.15}$$

which yields

$$(1 + s^2/N^2)^{\frac{3}{2}}(1 - 1/st) = n\pi V/N. \tag{3.16}$$

The front of the disturbance for mode n can be expected (from group-velocity considerations) to travel with the speed

$$V \simeq N/n\pi; \tag{3.17}$$

and it may readily be shown (by the saddle-point method or otherwise) that

$$I \begin{cases} \simeq 0 & \text{for} \quad V \gg N/n\pi, \\ = 1 & \text{for} \quad V \ll N/n\pi. \end{cases} \tag{3.18}$$

Hence we write

$$V = (N/n\pi)(1+\gamma) = P(1+\gamma), \tag{3.19}$$

assuming $|\gamma| \ll 1$ at first. Formally this suggests that $s^2/N^2 \ll 1$, and using this approximation in (3.16) yields

$$\frac{3}{2}\left(\frac{s}{N}\right)^3 - \frac{3}{2Nt}\left(\frac{s}{N}\right)^2 - \frac{\gamma s}{N} - \frac{1}{Nt} = 0. \tag{3.20}$$

This cubic equation may be solved conventionally, and writing

$$\gamma = 3^{\frac{4}{3}}B/(2(Nt)^{\frac{2}{3}}), \tag{3.21}$$

the three roots s_1, s_2 and s_3 are given by

$$\left.\begin{aligned} s_1/N &= \beta_1(2Nt)^{-\frac{1}{3}}[1+O((Nt)^{-\frac{2}{3}})], \\ s_2/N, s_3/N &= -\tfrac{1}{2}(2Nt)^{-\frac{1}{3}}(\beta_1 \pm i3^{\frac{1}{2}}\beta_2)[1+O((Nt)^{-\frac{2}{3}})], \end{aligned}\right\} \tag{3.22}$$

where

$$\left.\begin{aligned} \beta_1 &= [1+(1-B^3)^{\frac{1}{2}}]^{\frac{1}{3}} + [1-(1-B^3)^{\frac{1}{2}}]^{\frac{1}{3}}, \\ \beta_2 &= [1+(1-B^3)^{\frac{1}{2}}]^{\frac{1}{3}} - [1-(1-B^3)^{\frac{1}{2}}]^{\frac{1}{3}}. \end{aligned}\right\} \tag{3.23}$$

These are plotted in figure 2. Hence, provided that $Nt \gg 1$ and $B = O(1)$, s^2/N^2 is indeed small and the above approximations are valid. Only one saddle point has a positive real part, and this makes the greatest contribution to I, from which (Morse & Feshbach 1953, p. 438)

$$I = e^{tf(s_1)}/(2\pi t f(s_1))^{\frac{1}{2}} \tag{3.24}$$

$$= \exp(-\tfrac{3}{2}B\beta_1 + \tfrac{3}{4}\beta_1)/[\pi(3\beta_1^3+2)]^{\frac{1}{2}}, \tag{3.25}$$

with (3.21) and (3.22). The form of this equation as a function of B is plotted in figure 3. I_1 grows from very near zero to very near unity within the range $-1{\cdot}2 < B < 1{\cdot}0$, and so the form of the travelling wave is almost completely described within the range of the above approximations. For the tank and stratification used $Nt \simeq 18$ when the front for mode $n = 1$ arrives at the test section, which value is sufficiently large to justify the use of the above asymptotic analysis. The above structure is similar to that for a front in surface gravity waves, e.g. Jeffreys & Jeffreys (1962).

As B becomes more negative the saddle points s_2 and s_3 approach the imaginary axis, and we may write $I = I_1 + I_2 + I_3$, where I_1, I_2 and I_3 represent the contributions from the three saddle points.

When $|B| = O(1)$,

$$\left.\begin{aligned} |I_2+I_3| &= O(\exp-[\tfrac{1}{2}(2Nt)^{\frac{2}{3}}\beta_1 + \tfrac{3}{4}\beta_1]), \\ \text{while for } B \ll -1, \quad |I_2+I_3| &= O((x/Nt)^{\frac{1}{2}}/(Nt)^{\frac{1}{2}}). \end{aligned}\right\} \tag{3.26}$$

The term $I_2 + I_3$ represents oscillations which only become significant when the front of the motion has passed, and then decay with time according to (3.26).

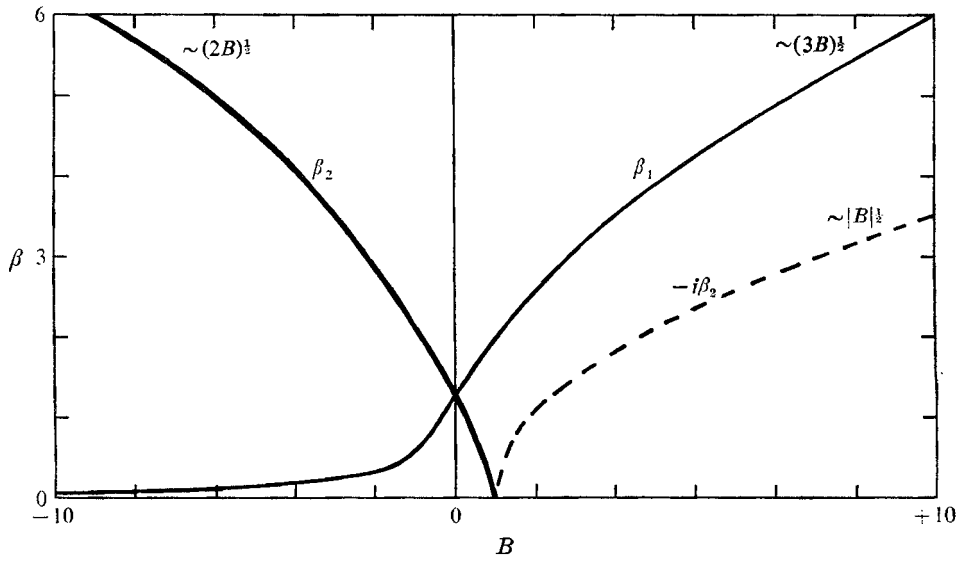

FIGURE 2. Parameters β_1 and β_2 defining the roots of (3.20).

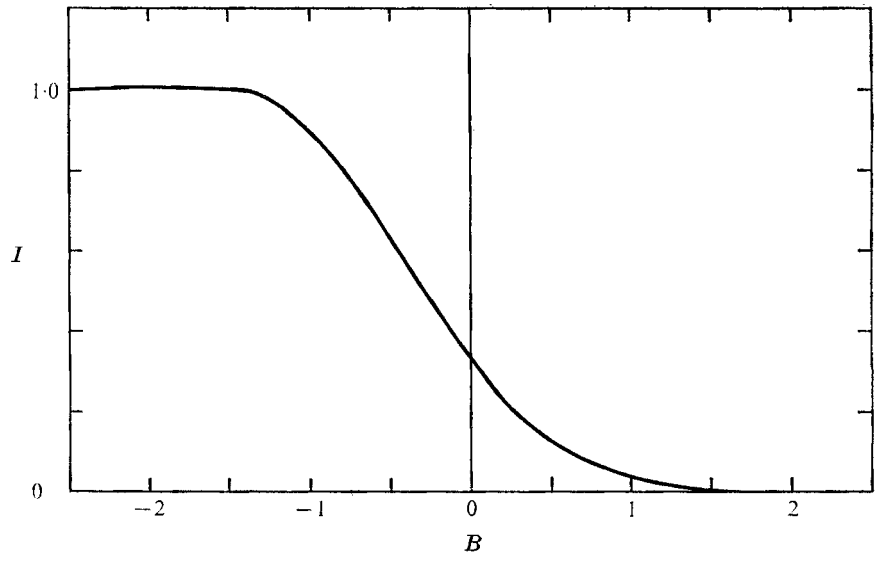

FIGURE 3. The profile of I defining the amplitude of horizontal shearing motion through the frontal region. For definitions see (3.13), (3.19) and (3.21).

Under present experimental conditions the theoretical amplitude of these oscillations (associated with the $n = 1$ mode) at the mid-point of the tank was never greater than 4 % of the contribution from I_1 (the basic shear).

To investigate the effect of initially angled paddles, we consider the geometry shown in figure 4(*a*) with boundary conditions as given by (3.5) and (3.10), except that the left-hand boundary condition is applied at

$$x = (\tfrac{1}{2} - z)\cot\theta, \tag{3.27}$$

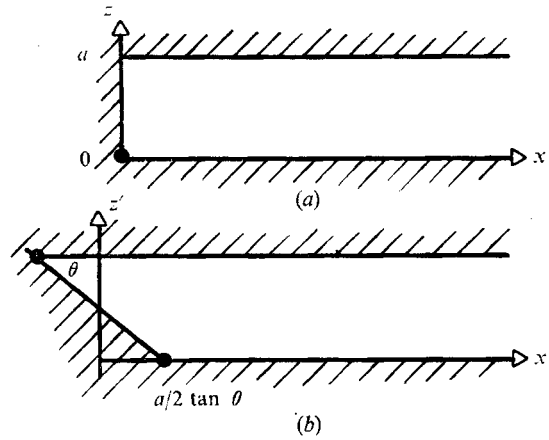

FIGURE 4. Transformation of co-ordinates for an inclined paddle.
(*a*) ξ plane. (*b*) η plane.

rather than at $x = 0$. Taking s to be real, the solution to (3.10) under these conditions may be obtained from the above solution via a Schwarz–Christoffel transformation. If we write

$$\xi = x + iz, \quad \eta = x' + iz',$$

where (x,z) and (x',z') are vertical and angled co-ordinates respectively (figure 4), then the appropriate transformation (Milne-Thomson 1960, p. 266) yields

$$\frac{d\eta}{d\xi} = \frac{k}{1+\cosh \pi\xi}\left(\frac{\cosh \pi\xi + 1}{\cosh \pi\xi - 1}\right)^{\theta/\pi}, \tag{3.28}$$

where k is a constant depending on θ. Consider the case $\theta = \frac{1}{3}\pi$. Integrating (3.28) and matching at the corners gives $k = 1/\pi$, and for x large

$$\frac{x'}{\mu} + iz' = \frac{x}{\mu} + iz + \frac{\log(\frac{3}{4}\times 3^{\frac{1}{2}})}{\pi} - \tfrac{7}{6}\exp\left[-\pi(x/\mu + iz)\right] + O(e^{-2\pi x/\mu}), \tag{3.29}$$

so that

$$\frac{x}{\mu} + iz = \frac{x'}{\mu} + iz' - \frac{\log(\frac{3}{4}\times 3^{\frac{1}{2}})}{\pi} + \frac{7\times 3^{\frac{1}{2}}}{8}\exp -\pi(x'/\mu + iz') + O(e^{-2\pi x/\mu}). \tag{3.30}$$

For $\mathrm{Re}\, s > 0$ it is readily shown that $\mathrm{Re}\,\mu > 0$ on the appropriate branch.

Hence, apart from a constant factor affecting only the magnitude of each mode of the solution, the form of the wave (for the $n = 1$ mode in particular) for x large will be given by substitution of (3.30) in (3.12). An initially angled wave front becomes vertical as the wave propagates down the channel, in a distance comparable with the depth.

The motion of a single paddle therefore results in a set of odd internal wave modes of zero frequency each travelling down the channel behind a front of width $O(n^{-1}(Nt)^{\frac{1}{3}})$, which travels at the appropriate group velocity, $P = N/n\pi$. The motion is essentially linear, since the advective and inertial terms are small, although the horizontal velocities behind the front may be large.

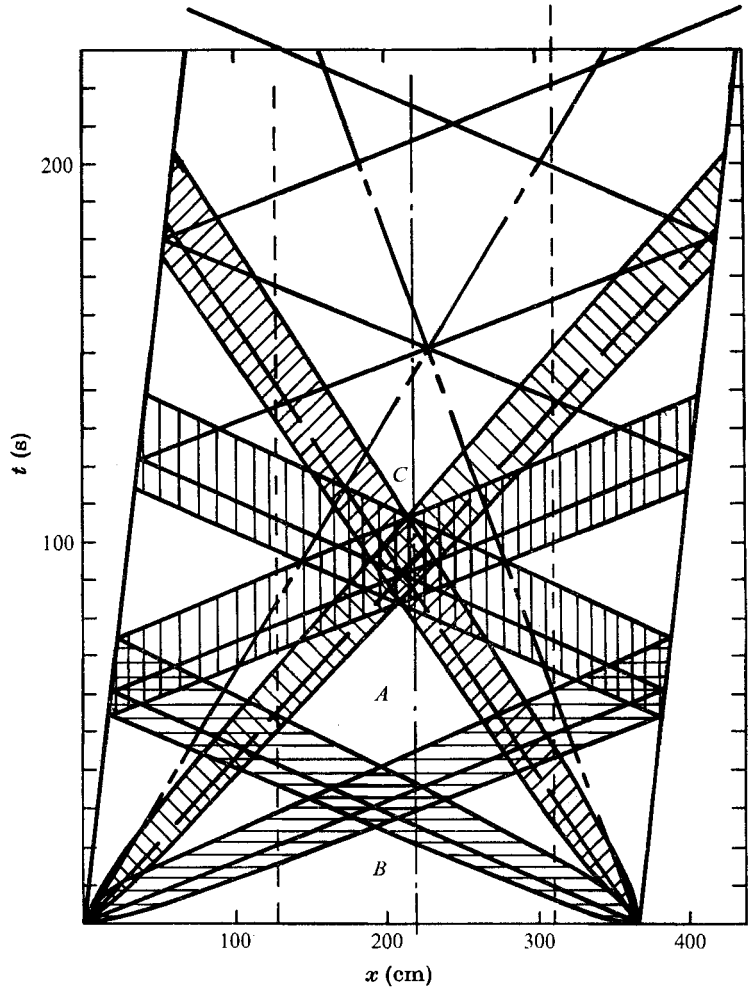

FIGURE 5. Frontal propagation represented by x, t diagram. ≡≡≡, positive primary-mode ($n = 1$) fronts originating at initial mean positions of the paddles; |||||, reflected negative $n = 1$ front; //////, positive $n = 3$ fronts; region A, steady shear region; region B, shearing motion region in tilting tube device. At point C the $n = 1$ mode has been annihilated by reflected negative fronts; the residual motion is barotropic flow plus $n = 3$ shear.

In the experimental channel, fronts for the first modes from each end meet near the centre and pass through one another leaving a superposition of sinusoidal shear flow profiles. The process is conveniently represented on an x, t diagram (figure 5). On this figure the origin of the front is located at the mid-point of the paddle, and the barotropic motion is then shown by a diagonal rightward shift of the frame relative to which the fronts move at rate $\frac{1}{2}\alpha$, where α is paddle shear. The front region, over which the strength function I increases from 0·1 to 0·9, is shown by horizontal hatching, and grows in width with time according to (3.19) and (3.21). On arrival at the opposing paddle, each front is reflected and re-crosses the central region. If there is no attenuation in frontal strength, the primary-mode ($n = 1$) shear in that region is annihilated. However, coincident with the

intersection of the reflected primary mode the $n = 3$ mode (whose frontal region is marked by diagonal hatching) arrives, so that shortly after time C the residual motion in the central region comprises the barotropic component plus an $n = 3$ shearing mode.

Thus on figure 5 the primary region in which a usable steady experimental shear of primary mode only is sustained is region A. In comparison, the accelerating shear region using the Thorpe technique with the same channel geometry would be approximately represented by region B.

Also shown on figure 5 are lines giving the centre of the $n = 5$ mode front, which arrives well after the experimentally useful period; thus approximately triangular shear is achieved only after a long time; unless the shearing rate is very low this time exceeds that for the paddles to reach their limit of travel.

It should be noted that with this technique with constant N the Richardson numbers attainable are limited to $Ri > \frac{1}{4}$, since

$$(du/dz)_{\max} = 8\alpha/\pi,$$

and we require that the paddle speed at the surface (relative to translating axes) be less than the frontal speed, which implies that

$$\tfrac{1}{2}\alpha < N/\pi,$$

so that

$$Ri > (\tfrac{1}{4}\pi)^4 \simeq 0{\cdot}38.$$

However, the procedure is not restricted to constant stratification, and it is readily seen by analogy with the above theoretical argument that the shear profiles following the fronts will be those appropriate to long internal gravity waves for that density gradient. By choosing the density gradients appropriately, low Richardson numbers may be realized more easily, and even $Ri < \frac{1}{4}$ achieved when the waves from each end superimpose.

4. Experimental evaluation

Figure 6 gives representative horizontal velocity profiles measured at the mid-plane for a paddle shearing rate of 1·07 cm/s and depth of 32·1 cm, with a stratification N of 0·63 rad/s over the central 80 % of the depth. Owing to diffusion and thermal convection the stratification weakened towards zero in the top 10 % and the bottom 5 % of the depth. As shown in the appendix these defects were expected to exert a negligible influence on the shear flow structure. Velocities given in the figure are derived from photographic time exposures, about 5 s in duration, of neutrally buoyant polystyrene beads dispersed throughout the liquid.

The figure shows that as time proceeds the initially barotropic motion is replaced by a growing half-sinusoidal ($n = 1$) shear, which then weakens concurrently with the arrival of $n = 3$ mode motion (q.v., figure 5).

Figure 7 compares the results of a number of tests under similar conditions with paddle shears α varying over a range from 0·0079 to 0·119 s^{-1}. As for the previous figure N was 0·63 s^{-1}. The results are the amplitude of the primary, $n = 1$, mode expressed as a fraction of its theoretical maximum value $8\alpha/\pi$, given by (3.7) and (3.8). The theoretical time variation of this mode is shown by

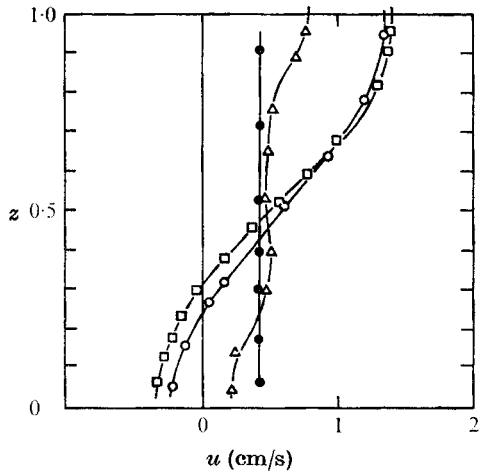

FIGURE 6. Horizontal velocity profiles at various times measured at mid-plane; paddle shear $\alpha = 0{\cdot}0333\,\mathrm{s}^{-1}$; $N = 0{\cdot}63\,\mathrm{s}^{-1}$, minimum Richardson number = 54. ●, $t = 2{\cdot}7$ s; barotropic motion only; ○, $t = 35{\cdot}2$ s, within the $n = 1$ shear front; □, $t = 67{\cdot}4$ s, fully developed $n = 1$ shear; △, $t = 107$ s, attenuating $n = 1$ shear, plus $n = 3$ shear.

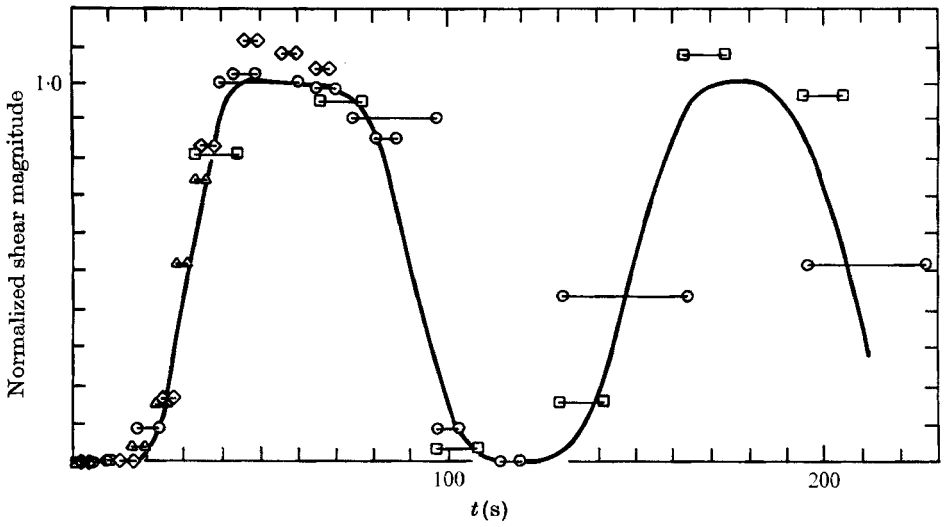

FIGURE 7. Shear amplitude *vs.* time. Shears normalized by $8\alpha/\pi$. ——, theoretical variation. Experiments, $N = 0{\cdot}63\,\mathrm{s}^{-1}$: ●, $\alpha = 0{\cdot}0079\,\mathrm{s}^{-1}$; □, $\alpha = 0{\cdot}018\,\mathrm{s}^{-1}$; ○, $\alpha = 0{\cdot}0333\,\mathrm{s}^{-1}$; ◇, $\alpha = 0{\cdot}065\,\mathrm{s}^{-1}$; △, $\alpha = 0{\cdot}119\,\mathrm{s}^{-1}$. Bars indicate the period over which measurements are averaged.

the solid line, derived using (3.17), (3.19), (3.21), (3.23) and (3.25) and assuming the reflexion scheme of figure 5.

The experimental results were derived from the difference between velocities at the top and the bottom of the channel with higher mode contributions subtracted. Direct shear measurement was susceptible to errors near the zero velocity position owing to weak residual barotropic unsteadiness. On the figure the bars indicate the period over which the motion was averaged. The speed and

strength of the shear front is generally in good agreement with theory over the whole experimental period. One test, for unknown reasons, gave frontal strengths about 11 % higher than the predicted maximum.

5. The effect of a contraction

If a vertical-sided two-dimensional contraction is introduced into the channel, as shown in figure 1, the vertical velocity may be written as

$$w(x, y, z, t) = \overline{w}(x, y, t) \sin n\pi z, \tag{5.1}$$

on the assumption that the vertical structure of the motion is retained. From the equations of motion with the previously used approximations

$$\nabla^2 w_{tt} + N^2 \nabla_H^2 w = 0, \tag{5.2}$$

where $\nabla^2 \equiv \partial^2/\partial x^2 + \partial^2/\partial y^2 + \partial^2/\partial z^2$, $\nabla_H^2 \equiv \partial^2/\partial x^2 + \partial^2/\partial y^2$.

Then, substituting (5.1),

$$(\partial^2/\partial t^2 + N^2) \nabla_H^2 w - n^2\pi^2 \overline{w}_{tt} = 0. \tag{5.3}$$

By inspection it can be seen that as $N^2 \gg \partial^2/\partial t^2$ this equation reduces to the wave equation in two dimensions:

$$\nabla_H^2 \overline{w} - (n^2\pi^2/N^2) \overline{w}_{tt} = 0, \tag{5.4}$$

in which disturbances are propagated at a uniform speed $P = N/n\pi$ independent of horizontal direction. By applying (3.19) and (3.21) for flow prior to arrival at the contraction it is found that $N^2/(\partial^2/\partial t^2)$ is $\frac{9}{10}(Nt)^2$, or for the first arrival of the front at the channel contraction, a value of about 100. Equation (5.4) indeed applies and the frontal behaviour can be likened to that of a diffuse sonic disturbance. Angles of incidence and reflexion at the contraction walls are equal and the proportion of the incident front finding its way through the narrowed section can be estimated by geometry, as follows.

Consider the arrival of a front comprising an individual shear mode n of magnitude G_n as given by (3.8), and a contraction of ratio (least/greatest width) W and angle θ to the incident propagation direction. Part of the front travels directly into the narrow section without being deflected by the contraction walls. This part has unaffected amplitude G_n (denoted by F_0 here) and speed

$$P\ (= N/n\pi).$$

The remainder of the front is reflected by the contraction and channel walls. After each reflexion on the channel wall the angle of the propagation direction or ray of a given part of the front is increased by 2θ. If, after successive reflexions, this angle exceeds $\frac{1}{2}\pi$, that part of the front will not find its way into the narrow region and will ultimately be reflected back. Thus, for transmission the number of reflexion pairs K of a given ray is limited to

$$K < \pi/4\theta. \tag{5.5}$$

If this condition is not satisfied for all incident rays, by continuity it can be shown that F_K, the magnitude of a shear front within the narrow channel produced by

a section of incident front which has experienced K reflexion pairs (where K satisfies (5.5)), is

$$F_K = G_n \prod_{J=1}^{J=K} \left[\frac{\tan 2J\theta + \tan\theta}{\tan 2J\theta - \tan\theta}\right] - \sum_{J=0}^{K-1} F_J, \tag{5.6}$$

and, necessarily,

$$\sum_{K=0}^{K_{\max}} F_K < G_n/W, \tag{5.7}$$

where $K_{\max}$ is the largest value of K for rays satisfying (5.5). There is a back-reflected front (or fronts) of total amplitude

$$W \sum_{K=0}^{K_{\max}} F_K - G_n.$$

If (5.5) is satisfied for all incident rays, the magnitude of F_K is given by (5.6) if $0 < K < K_{\max}$; (5.7) is now an equality, and this determines $F_{K_{\max}}$.

In reality all of these frontal 'sections' are connected by diffraction regions, so that each is eroded in strength as time proceeds. In addition each transmitted section F_K has a reduced net propagation velocity $P\cos(2K\theta)$ down the narrow channel. As a result the transmitted frontal region becomes rapidly diffused, and the above description based on the geometry of rays should only be regarded as a useful guide.

Note that, for $22{\cdot}5° < \theta < 45°$, by the above equations

$$\left.\begin{aligned} &K \leqslant 1, \quad F_0 = G_n, \\ F_1 = &\begin{cases} 2G_n\cos 2\theta & \text{if} \quad W^{-1} > 2\cos 2\theta + 1, \\ G_n/W - G_n & \text{if} \quad W^{-1} < 2\cos 2\theta + 1. \end{cases} \end{aligned}\right\} \tag{5.8}$$

An 'optimum' contraction, one in which the minimum value of W is attained for a given θ *without back reflexion*, is determined by the condition

$$W^{-1} = 2\cos 2\theta + 1, \quad \tfrac{1}{8}\pi < \theta < \tfrac{1}{4}\pi.$$

Optimization is possible for lower values of W by admitting higher K sections of the incident front, but this requires $\theta < 22{\cdot}5°$, and results in a larger dispersion of the transmitted front. Thus for practical purposes little benefit is gained by having $\theta < \frac{1}{8}\pi$ and $W < 1/(1+2^{\frac{1}{2}})$.

To relate the foregoing to experiments only a crude comparison is justified, since in addition to the neglect of diffraction, there exist unpredictable effects arising from boundary-layer separation at the exit. Furthermore, within the narrowed channel, boundary-layer growth can be inconvenient; the 90% velocity thickness of a wall layer originating at the paddle and growing from zero thickness in an impulsively started flow is about $1{\cdot}16(4\nu t)^{\frac{1}{2}}$ (Rosenhead 1963, equation VII, 25), where ν is the kinematic viscosity. 50 s after frontal passage boundary layers have penetrated more than 1·6 cm on each side.

In the experiments $\theta \simeq 20°$ so for practical purposes (5.8) apply; the front was taken to be composed of a plane front of strength G_1 travelling at speed $P = N/\pi$ followed by a single front of strength F_1 travelling at speed $P\cos(2\theta)$. No allowance was made for boundary layers.

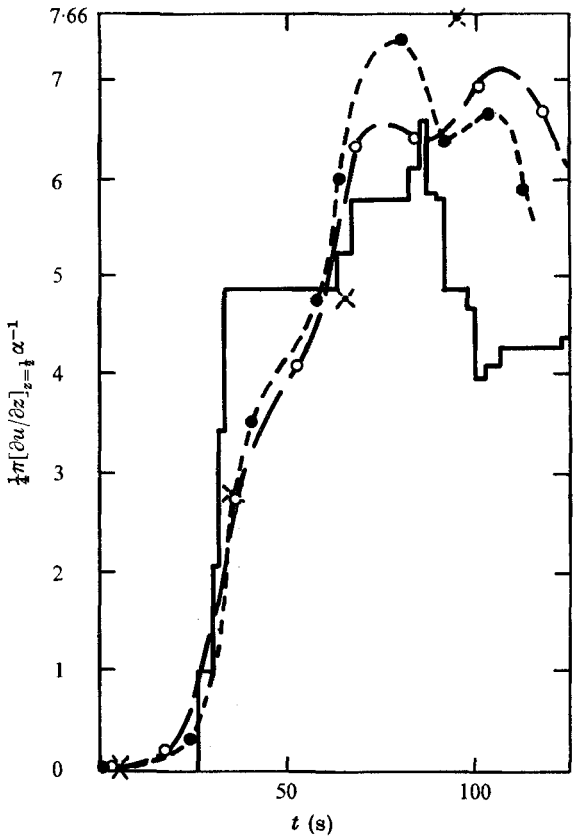

FIGURE 8. Shear amplitude (normalized by α) *vs.* time within a contraction 0·26 of channel width. ——, theoretical amplitude with shear fronts represented by step changes. Points and broken lines: experiment $N = 0{\cdot}63\,\mathrm{s}^{-1}$. ×, $\alpha = 0{\cdot}0086\,\mathrm{s}^{-1}$; ○, $\alpha = 0{\cdot}0182\,\mathrm{s}^{-1}$; ●, $\alpha = 0{\cdot}0342\,\mathrm{s}^{-1}$.

Figure 8 shows experimental measurements of shear strength within a contraction shaped as shown in figure 1, for which $W = 0{\cdot}26$, $\theta = 21{\cdot}8°$. Using (5.8) we have $F_0 = G_n$ and $F_1 = 1{\cdot}45G_n$, with G_n given by (3.8). The back-reflected front has strength $-0{\cdot}36G_n$, i.e. it weakens the shear arriving at the contraction. This latter front is reflected at the paddle, becoming a positive front, and transmits $0{\cdot}36 \times 2{\cdot}45G_n$ into the contraction after re-arrival. In the figure, theoretical fronts are represented as steps of appropriate strength, normalized with respect to G_n.

Because of the repeated back reflexion the shear strength is never steady for an appreciable length of time; the theoretical line (not taking diffraction into account) shows little resemblance to the experimental results, which have a double hump of shear strength with time. The disparity can be qualitatively explained by diffraction effects. These are revealed more clearly with an 'optimized' contraction, for which $F_1(\theta) = W^{-1}\,G_n$, there being, then, according to (5.8) no back reflection. Figure 9 shows results of such a contraction for which $W = 0{\cdot}389$ and $\theta = 19{\cdot}2°$. The theoretical (undiffracted) front reaches a plateau,

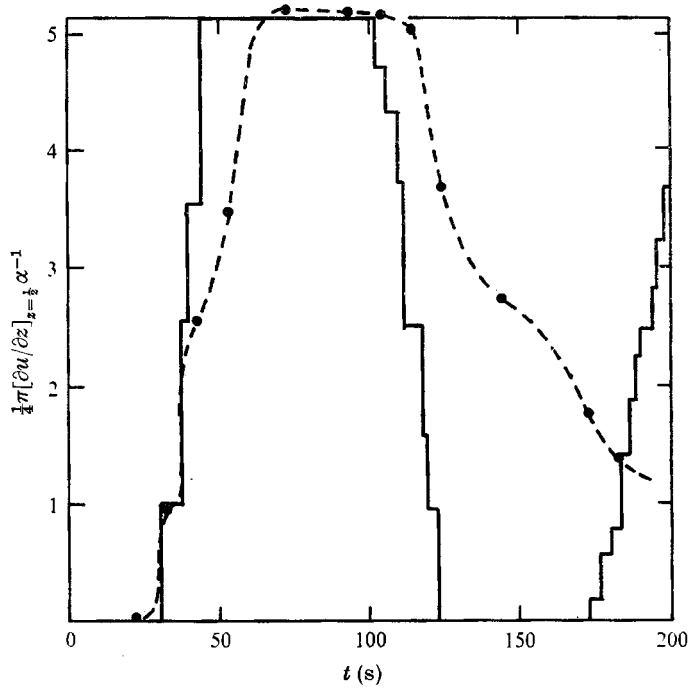

FIGURE 9. Shear amplitude (normalized by α) *vs.* time within an 'optimized' contraction 0·39 of channel width. ——, theoretical amplitude with shear fronts represented by step changes; – – ● – –, experiment, $N = 0{\cdot}515\,\mathrm{s}^{-1}$, $\alpha = 0{\cdot}0165\,\mathrm{s}^{-1}$.

and is then annihilated by the returning negative front, as is the case (figure 7) when the contraction is absent. Experimental shears also reach a plateau of useful duration corresponding well in strength with theoretical estimates. In support of predictions, there is no sign of repeated back reflexion. Effective frontal propagation lags in speed by 20 % or more behind that derived neglecting diffraction, and clearly for accurate prediction a proper calculation based upon (5.4) would have to be undertaken.

6. Conclusion

Baroclinic disturbances generated by a sudden change in velocity at the end boundary of a layer of uniform stratification generate a set of modes n which propagate at a speed $P = Nh/n\pi$, where N is the buoyancy frequency and h is the layer depth. The resultant changes in horizontal fluid motion are nearly monotonic and confined within a weakly dispersive 'front' of width $O((h/n)(Nt)^{\frac{1}{2}})$. The speed P is, to first order, independent of the modal strength and the propagation and reflexion properties of these fronts are similar to those of infinitesimal sonic disturbances. Imperfections in stratification of thickness h_i effect changes of only $O((h_i/h)^3)$ in the transmission of the fronts and the profile and strength of the following shear.

In relation to the experimental shear flow device described, the theory may

be applied to predict accurately the duration and strength of shears produced. The shear strength is twice the magnitude of that applied to the paddle generators, and can be sustained for a period nearly twice as long as that attainable in a tilting tube device of the same geometry.

Since the upper surface is free there are also operational advantages over the tilting tube in accessibility to models placed in the channel, and in the ability to repeat experimental runs. The device is mechanically simpler than other shear flow apparatus.

To strengthen the shear, contractions may be inserted into the channel, but require suitable design to ensure that flow steadiness is not sacrificed. Because of refraction and repeated reflexion the shear front is strongly dispersed by contractions, and there exists a practical limit to the contraction ratio.

Appendix. The effect of stratification imperfections

Imperfections always arise in laboratory preparation of a stratified medium; thermal convection by evaporation or ambient temperature variation is effective in weakening density gradients near the top and bottom of a tank filled with stratified salt solution, but in addition molecular diffusion near these boundaries will produce weakened layers $O((\kappa t)^{\frac{1}{2}})$ thick, κ being the salt diffusion coefficient.

To investigate their effects on the foregoing analysis, we consider a stratification $N(z)$ as follows:

$$N = \begin{cases} 0, & 0 < z < h_1, \\ N, & h_1 < z < 1-h_2, \\ 0 & 1-h_2 < z < 1, \end{cases} \tag{A 1}$$

and write $\psi = \overline{\psi}(z)\, e^{i(kx-\omega t)}$. Hence

$$\overline{\psi}_{zz} + m^2 \overline{\psi} = 0, \tag{A 2}$$

where $m^2(z) = k^2(N^2/\omega^2 - 1)$. Thus

$$\overline{\psi} = \begin{cases} A \sin mz + B \cos mz, & h_1 < z < 1-h_2, \\ Cz, & 0 < z < h_1, \\ D(1-z), & 1-h_2 < z < 1, \end{cases} \tag{A 3}$$

where kh_1 and kh_2 are assumed small By matching ψ and the pressure across interfaces h_1 and $1-h_2$ we find, after manipulation to eliminate C and D,

$$A(mh_1 - \tan mh_1) - B(1 + mh_1 \tan mh_1) = 0, \tag{A 4}$$

$$A[mh_2 + \tan m(1-h_2)] + B[1 - mh_2 \tan m(1-h_2)] = 0. \tag{A 5}$$

Regarding mh_1, $mh_2 \ll 1$, and taking $\tan \epsilon \simeq \epsilon + \frac{1}{3}\epsilon^3$, $\epsilon \ll 1$,

$$B \simeq -\tfrac{1}{3} A (mh_1)^3 [1 + O((mh_1)^2)]. \tag{A 6}$$

Then substituting in (A 5), with the same approximation, we obtain

$$\tan m \simeq \tfrac{1}{3}[(mh_1)^3 + (mh_2)^3], \quad m \simeq \pi + \tfrac{1}{3}\pi^3 (h_1^3 + h_2^3). \tag{A 7}$$

The boundary conditions then give

$$C = A[1 + O(\pi h_1)^2], \quad D = \pi A[1 + O(\pi h_2)^2]. \tag{A 8}$$

The change in modal structure in the stratified region is thus of third order in h_1 and h_2.

The effects of the change in density structure on the amplitudes of the modes may be examined by evaluating their coefficients in a Fourier expansion (the modes are orthogonal to $O(h_1^3, h_2^3)$), and this yields, after some algebra, that the amplitudes are only altered by a term which is again $O(h_1^3, h_2^3)$.

REFERENCES

HEWETT, T. A., FAY, J. A. & HOULT, D. P. 1970 Laboratory experiments of smokestack plumes in a stable atmosphere. *M.I.T. Mech. Engng. Dept. Fluid Mech. Lab. Publ.* no. 70–9.

JEFFREYS, H. & JEFFREYS, B. S. 1962 *Methods of Mathematical Physics*, 3rd edn, §17.09. Cambridge University Press.

MILNE-THOMSON, L. M. 1960 *Theoretical Hydrodynamics*, 4th edn. Macmillan.

MOORE, H. J. & LONG, R. R. 1971 An experimental investigation of turbulent stratified shearing flow. *J. Fluid Mech.* **49**, 635.

MORSE, P. M. & FESHBACH, H. 1953 *Methods of Theoretical Physics*, vol. 1. McGraw-Hill.

ODELL, G. M. & KOVASZNAY, L. S. G. 1971 A new type of water channel with density stratification. *J. Fluid Mech.* **50**, 535.

OSTER, G. 1965 Density gradients. *Sci. Am.* **213**, 70.

ROSENHEAD, L. (ed.) 1963 *Laminar Boundary Layers*. Oxford University Press.

SCOTTI, R. S. & CORCOS, G. M. 1972 An experiment on the stability of small disturbances in a stratified free shear layer. *J. Fluid Mech.* **52**, 499.

THORPE, S. A. 1968 A method of producing a shear flow in a stratified fluid. *J. Fluid Mech.* **32**, 693.